ANALYSIS OF MIXED MODE CRACK GROWTH IN A SHIP HULL MATERIAL UNDER DYNAMIC LOADING

C. R. BARNES
J. AHMAD
M. F. KANNINEN

Stress Analysis and Fracture Section
Battelle, Columbus Laboratories

ABSTRACT

Research on fracture in HY-100 steel under mixed mode (Modes I and II), dynamic, elastic-plastic loading conditions is described. A combined experimental and finite element analysis effort was pursued. The analysis employed the $\tilde{J}$ criterion for fracture; a criterion which effectively generalizes the conventional J-integral to mixed mode and dynamic loading conditions. The experiments were performed with inclined-notch three-point-bend specimens of HY-100 steel. By coupling the experiments and finite element analyses, a fracture criterion based on a critical $\tilde{J}$ value was devised and verified.

INTRODUCTION

The fracture mechanics techniques needed for materials that fracture in a highly ductile manner must give explicit attention to the extensive plastic deformation surrounding the crack tip. Extensive crack tip plasticity has two effects. First, because of crack tip blunting, crack growth initiation requires greater loads than are predicted by linear elastic fracture mechanics analyses. Second, significant amounts of stable crack growth under rising load can precede fracture instability. To cope with these essentially inelastic processes, elastic-plastic fracture mechanics techniques are now being widely pursued [1]. This research builds upon these developments to provide the basis for fracture mechanics treatments under the more general conditions of concern to ship structures.

Current work in elastic-plastic fracture mechanics is largely confined to quasi-static loading conditions and to crack growth in the opening mode (Mode I). Yet, in an impact loaded ship structure, crack initiation could occur under dynamic conditions with a combination of both the opening mode and the sliding mode (Mode II). Thus, it is necessary to obtain a quantitative understanding of crack growth initiation, propagation and arrest under initial combined mode dynamic loading conditions. The research described here is aimed at developing this understanding through a program of integrated experimental and finite element analysis work. The objective is to provide the basis for the more general inelastic-dynamic fracture mechanics approach that is needed for Navy applications.

THE GENERAL APPROACH

In a critical survey of progress on elastic-plastic fracture mechanics, Kanninen, et al [1] found that most efforts are focused on the J-resistance

curve approach. Despite the fact that such approaches are inherently limited to small amounts of crack growth prior to fracture instability, they do provide a significant improvement over the conventional linear elastic fracture mechanics techniques. However, the current approaches are restricted to Mode I conditions under quasi-static loading. While a generalization of the J-integral valid for mixed mode and dynamic loading conditions exists, it has not previously been critically examined. Nevertheless, in view of the success that has been achieved with J and the complete lack of a viable alternative, this parameter, known as the $\hat{J}$-integral, was selected for use in this study. The mathematical basis for $\hat{J}$ and the manner in which it can be applied to elastoplastic dynamic fracture problems can be found in references [2], [3], and [4].

The experimental portion of the research described in this paper employed HY-100 steel three-point-bend specimens with slant edge cracks. The specimen configuration is shown in Figure 1. This configuration has a number of advantages for this research. First, crack initiation and propagation can be obtained for both quasi-static and dynamic loading in the same specimen geometry. Second, by varying the crack angle and the crack length, a range of Mode I and Mode II combinations can be achieved. Third, this specimen can be economically analyzed with a finite element method. Fourth, because of the constraint that arises in bending, the J-resistance curves obtained may be lower bound values that will provide conservative predictions when utilized for structural integrity assessments [1].

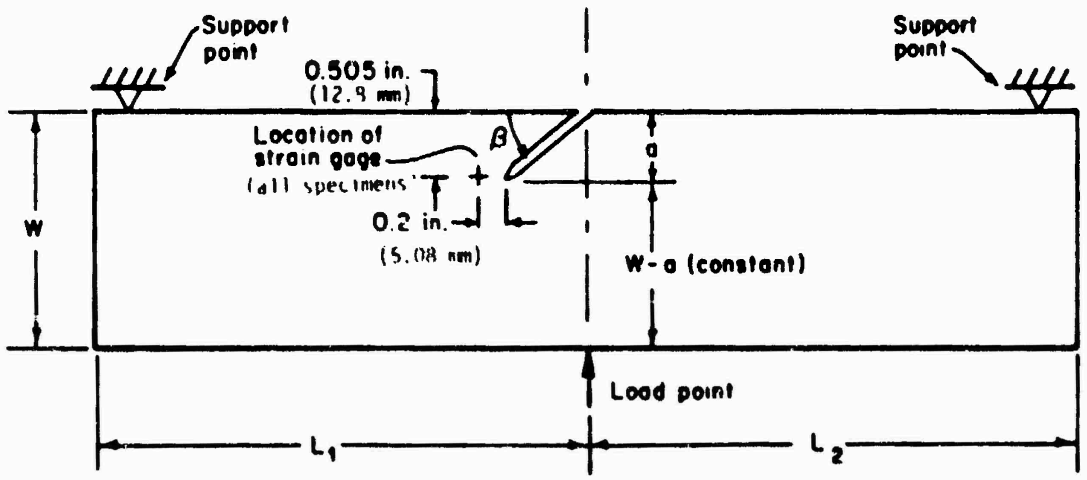

FIGURE 1. THREE-POINT-BEND SPECIMEN WITH A SLANT EDGE CRACK

A dynamic elastic-plastic finite element analysis was used in the analysis portion of the research. The objective was to learn if crack growth initiation in HY-100 steel is governed by critical values of $\hat{J}$. The $\hat{J}$ values were determined by finite element analyses of the experiments. In essence, by calculating the vectorial components of $\hat{J}$ (i.e., $\hat{J}_1$ and $\hat{J}_2$) as a function of load, and using the load level at initiation, critical values for

experiments performed with each different crack angle were determined. This provided a tentative elastic-plastic mixed mode fracture criterion in terms of a single material parameter.

Analyses were also performed for impact loading. Here, the fracture criterion deduced under quasi-static loading was used as input to a finite element simulation of the impact loaded experiment. In this way a prediction of the initiation time was made for comparison with an experiment. The quite reasonable accuracy of this prediction then gave an indication of the usefulness of the approach for the general conditions of interest in this research.

THE EXPERIMENTAL RESEARCH

Quasi-Static Loading Experiments

The specimen type used in this research was shown in Figure 1. Specimen blanks were cut from HY-100 steel plate. The chemical analysis and mechanical properties are shown in Tables 1 and 2. The specimen blanks were oriented such that the crack propagation direction for the specimens with $\beta = 90°$ (see Figure 1) was parallel to the plate rolling direction. Crack propagation in specimens with $\beta = 30°$ and $\beta = 45°$ was at 60° and 45°, respectively, to the rolling direction.

The general specimen configuration conformed with the ANSI/ASTM E604-77 Standard for Dynamic Tear Specimens except for the thickness and notch treatment. While the ANSI/ASTM standard [5] requires a thickness of 0.625 inch, 1.15-inch thick specimens (full plate thickness) were used in this investigation to promote plane strain behavior at the notch tip. The standard also requires that the notch root be sharpened by pressing a preformed tool into the notch root. However, past experience at Battelle has demonstrated that many otherwise ductile materials fail either partially or totally by cleavage when specimens containing the ANSI/ASTM specified notch are impact tested.

TABLE 1. HY-100 CHEMICAL COMPOSITION
(Average of Three Samples)

	C	Mn	P	S	Cu	Si	Ni	Cr	Mo	V	Ti
PLATE	.17	.30	.011	.017	.15	.28	2.76	1.51	.39	.003	.002
MIL (a) SPEC.	.12 to .20	.10 to .40	MAX. of .025	MAX. of .025	MAX. of .25	.15 to .35	2.25 to 3.50	1.00 to 1.80	.20 to .60	MAX. of .020	MAX. of .030

(a) Military Specification, Steel Plate, Alloy, Structural, High Yield Strength

(HY-80 and HY-100), MIL-S-1621H (SHIPS), (15 March 1972)

TABLE 2. HY-100 MECHANICAL PROPERTIES

Specimen Orientation	2% Offset Yield Strength (ksi)	Ultimate Tensile Strength (ksi)	Elongation (%)	Reduction of Area (%)	Modulus (10^6 psi)
Longitudinal (T-L)	107.6 (742Mpa)	121.3 (836Mpa)	20	72.4	31.8 (219Gpa)
Transverse (L-T)	108.1 (745Mpa)	121.8 (840Mpa)	20	70.3	31.1 (214Gpa)

(One such material is HY-100 steel). In addition, the specimen configuration precluded the use of fatigue to sharpen the notch root (as used in the ASTM standard for K_{Ic} specimens). Consequently, the notch was sharpened using a jeweler's saw that produced a root radius of about 3.25 mils. It was anticipated that this relatively blunt notch would store enough energy to promote rapid unstable crack propagation in the impact tests that are described later.

Table 3 lists the specimens tested under quasi-static loading conditions. Tests were performed using a Baldwin-Tate Emery Test Machine having a load capacity of 60,000 lbs. The loading rate was adjusted such that the load-point displacement (LPD) was 0.01 inch min^{-1}. The loading was interrupted at preselected points on the load-displacement curve to fill the notch with a silicone rubber compound. This procedure was used to determine the load at crack initiation. It was determined that the cracks initiated internally and tunnelled for a distance roughly equal to the shear lip width (0.2 to 0.3 inch) before reaching the surface.

TABLE 3. QUASI-STATIC LOADING EXPERIMENTS

Specimen Number	Crack Position	β	Maximum Load (lbs)
102S	Mid-Point	90°	39,000 (173.5 kN)
101S	"	45°	42,500 (189 kN)
103S	"	30°	43,000 (173.9 kN)

Specimen 101S ($\beta = 45°$) was further instrumented to determine strain versus load by means of a strain gage rosette. A crude verification of the strains was provided by a coarse grid applied to the specimen's opposite face. A photographic record of this grid was made at each load-strain increment. An identical grid was also applied to Specimen 103S ($\beta = 30°$) and photographically recorded. Figure 2 shows a montage of Specimen 103S from zero load to fracture. Figure 3 shows the fracture surfaces of all three specimens tested under quasi-static loading.

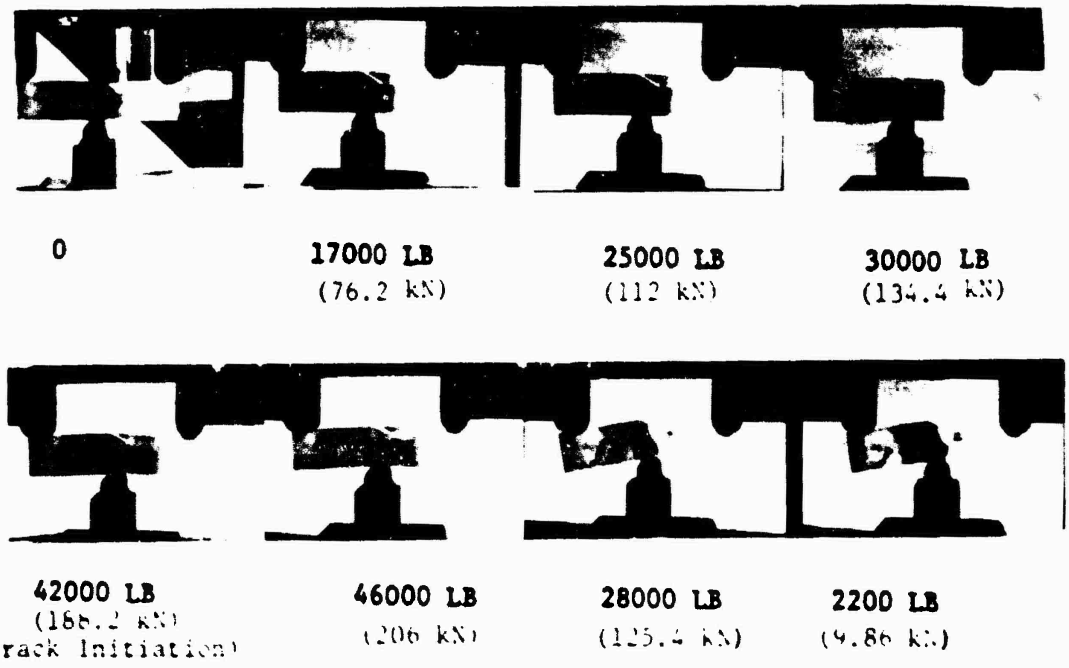

FIGURE 2. SPECIMEN 103S FROM ZERO LOAD TO FRACTURE

The experimental data from the three quasi-statically loaded specimens indicate the following. First, a plot of load versus load-point displacement (LPD) shows good agreement from specimen to specimen (Figure 4). The plot also indicates that lower values of β have higher values of the LPD at crack initiation. Second, the crack-tip-opening displacement (CTOD) at crack initiation was comparable in all specimens even though considerable data scatter was evident at lower loads (Figure 5). The source of this scatter was possibly caused by deformation zones observed about 4 mm from the crack tip.

β = 30° β = 45° β = 90°

FIGURE 3. FRACTURE SURFACES OF THE QUASI-STATICALLY LOADED SPECIMENS

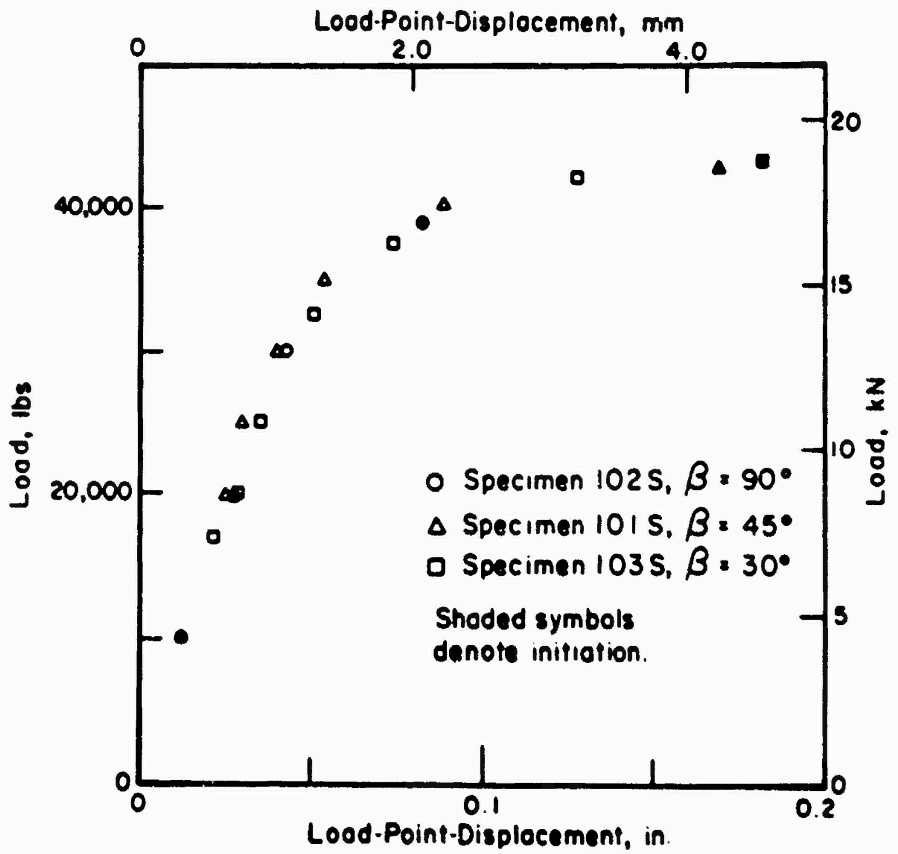

FIGURE 4. LOAD AS A FUNCTION OF LOAD-POINT-DISPLACEMENT FOR THE QUASI-STATIC LOADING EXPERIMENTS

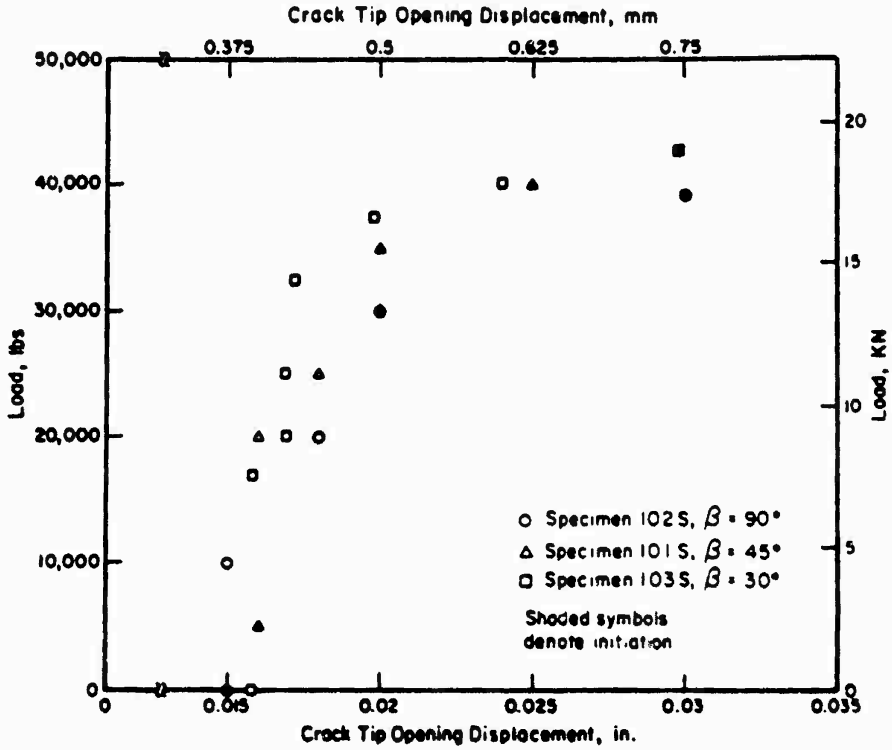

FIGURE 5. LOAD AS A FUNCTION OF CRACK TIP OPENING DISPLACEMENT FOR THE QUASI-STATIC LOADING EXPERIMENTS

Dynamic Loading Experiments

A Battelle designed and built machine, similar in concept to a Charpy machine, was used to conduct the impact tests. It is a multipurpose pendulum-type machine with a total impact energy of approximately 16,000 ft-lbs. A variety of specimen geometries can be accommodated by changing the bolt-on supports. Figure 6 shows a photograph of the specimen loading arrangement used in the tests.

To assess the practicality of determining crack initiation and crack propagation speeds in HY-100 steels, a crack monitoring gage was deposited upon a trial specimen surface according to the procedure given by Kanninen, et al [6]. This technique involves the vapor deposition of an electrically conducting grid upon a thin epoxy layer bonded to the test specimen surface. A strain gage was also applied to the specimen at the locations shown in Figure 7. In addition, the impact machine was electrically wired to indicate the time of the tup-specimen contact. The tup contact switch and output from

FIGURE 6. IMPACT LOADING ARRANGEMENT

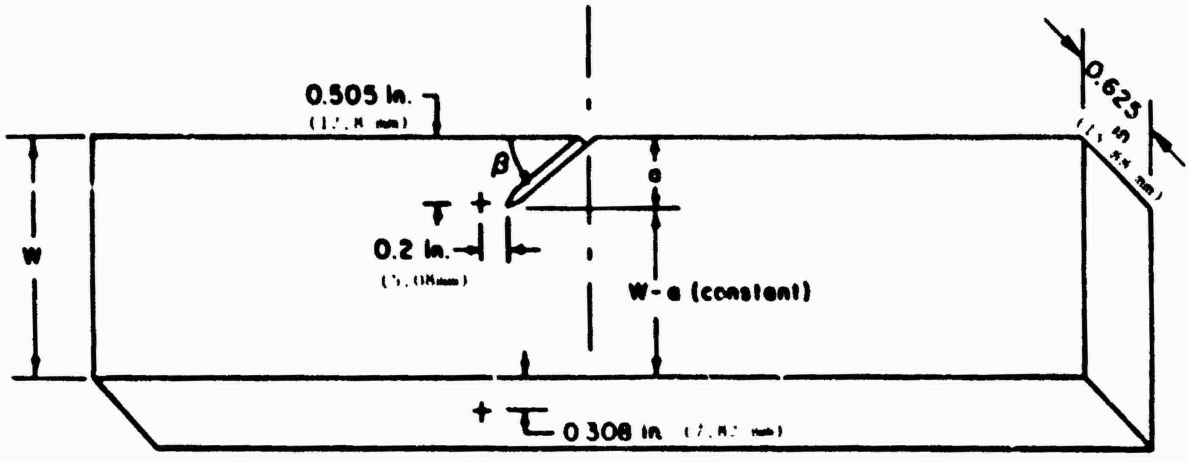

FIGURE 7. FEASIBILITY TEST SPECIMEN SHOWING STRAIN GAGE LOCATION

the crack monitoring gage were recorded simultaneously by a Biomation 8100 transient recorder and an FM tape recorder. The strain gage outputs were recorded on two adjacent tape channels.

Although the data from this feasibility test indicated that the dynamic initiation could be deduced (Figure 8), the crack speed record was less definitive. This was probably caused by the large plastic zone generated at the crack tip which resulted in epoxy-specimen separation. This condition rendered the speed measurement suspect since past experience has shown that it is essential that no epoxy-specimen debonding occurs for reliable crack speed determination. This, coupled with the suspicion that crack tunneling posed similar problems in determining the instant of crack initiation, prompted specimen modification for the impact tests. Accordingly, three specimens were prepared (one each with $\beta = 90°$, 45° and 30°) in which the notch configuration was altered as shown in Figure 9.

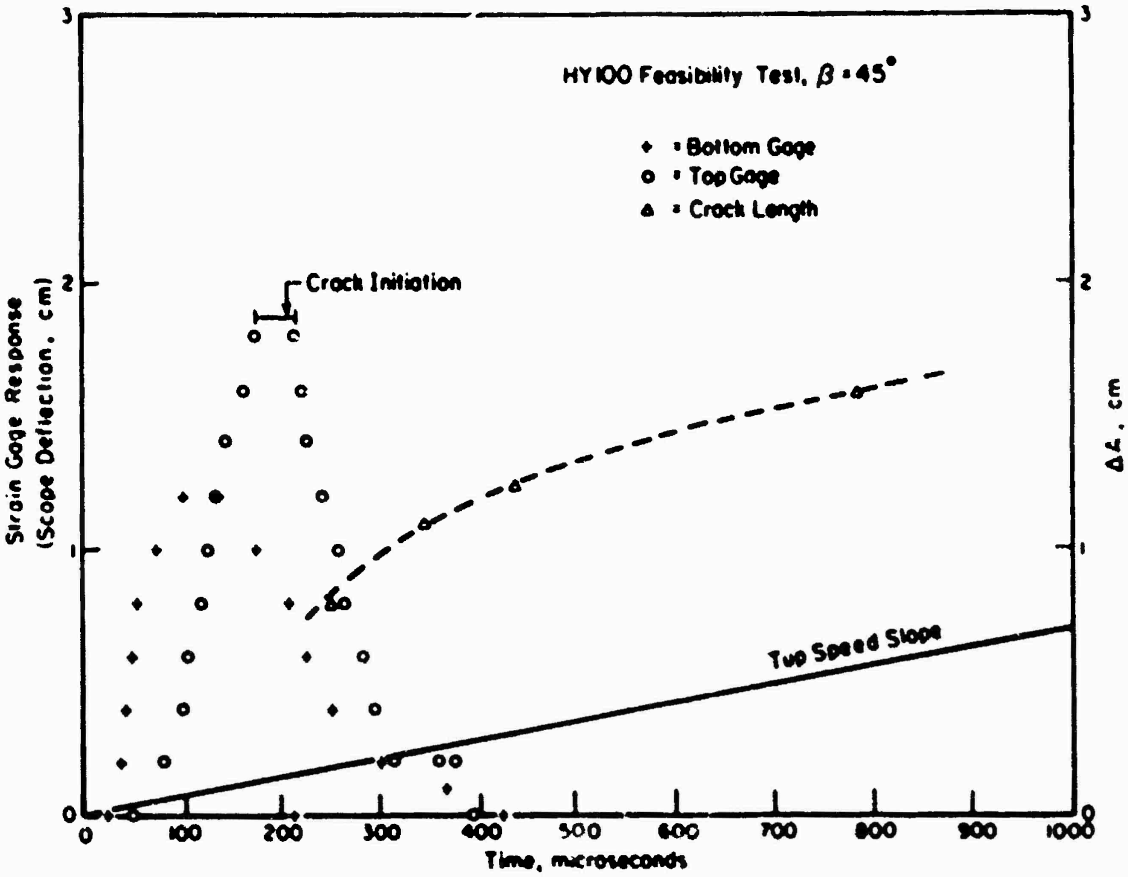

FIGURE 8. RESULTS OF IMPACT LOADED FEASIBILITY EXPERIMENT WITH $\beta = 45°$ (Time 0 = tup contact)

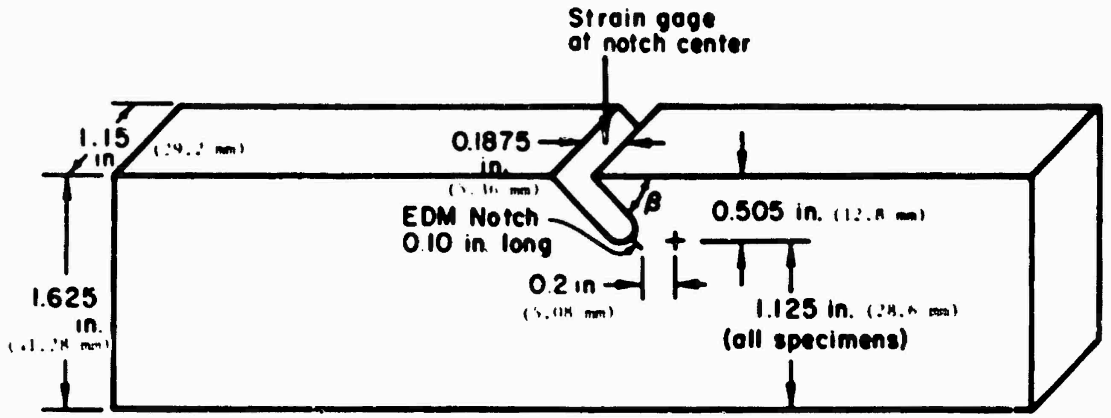

FIGURE 9. IMPACT SPECIMENS WITH CRACK STARTER NOTCH STRAIN GAGE APPLICATION

The notch geometry shown in Figure 9 was adopted so that a strain gage could be applied in the notch center. This indicates crack initiation more precisely than would a gage placed upon the specimen surface. Another gage was positioned at the side of the sharpened notch as in previous specimens. This gage was used to detect the time at which the internally initiated crack surfaced. As will be shown later, the crack initiation data agreed very well with the data from the feasibility test, which indicated that the crack surfaced at about 200 μsec. The surface crack initiation times for $\beta = 90°$, 45° and 30° were 230, 222, and 250 μsec, respectively. Note, however, that the feasibility test was conducted on a thinner specimen. Table 4 lists the three test specimens and the energy required to fracture them.

TABLE 4. IMPACT LOADED EXPERIMENTS

Specimen Number	Crack Position	β	Impact Energy (ft-lbs)
112D	Mid-Point	90°	1479 (2006 J)
113D	Mid-Point	45°	1982 (2688 J)
114D	Mid-Point	30°	1845 (2502 J)

THE ANALYSIS RESEARCH

The analysis effort in this research involved performing elastoplastic, quasi-static and dynamic finite element analyses of the experiments. The quasi-static analyses were performed to compute the $\hat{J}$ integral values corresponding to the experimentally determined loads at crack growth initiation. Using the $\hat{J}$ values at initiation under quasi-static loading conditions,

a crack initiation criterion was devised and used in the dynamic analyses for the prediction of crack initiation in impact loading.

All finite element analyses were performed using Battelle's elasto-plastic dynamic finite element fracture analysis computer code. The finite element meshes used in the analyses are shown in Figure 10. The numbered dotted lines in Figure 10 indicate the three contours used for computing the J-integrals. The values obtained using the three contours were found to be fairly path independent [4]. The results of the quasi-static analyses summarized in Table 5 represent the average of the three contours at initiation load.

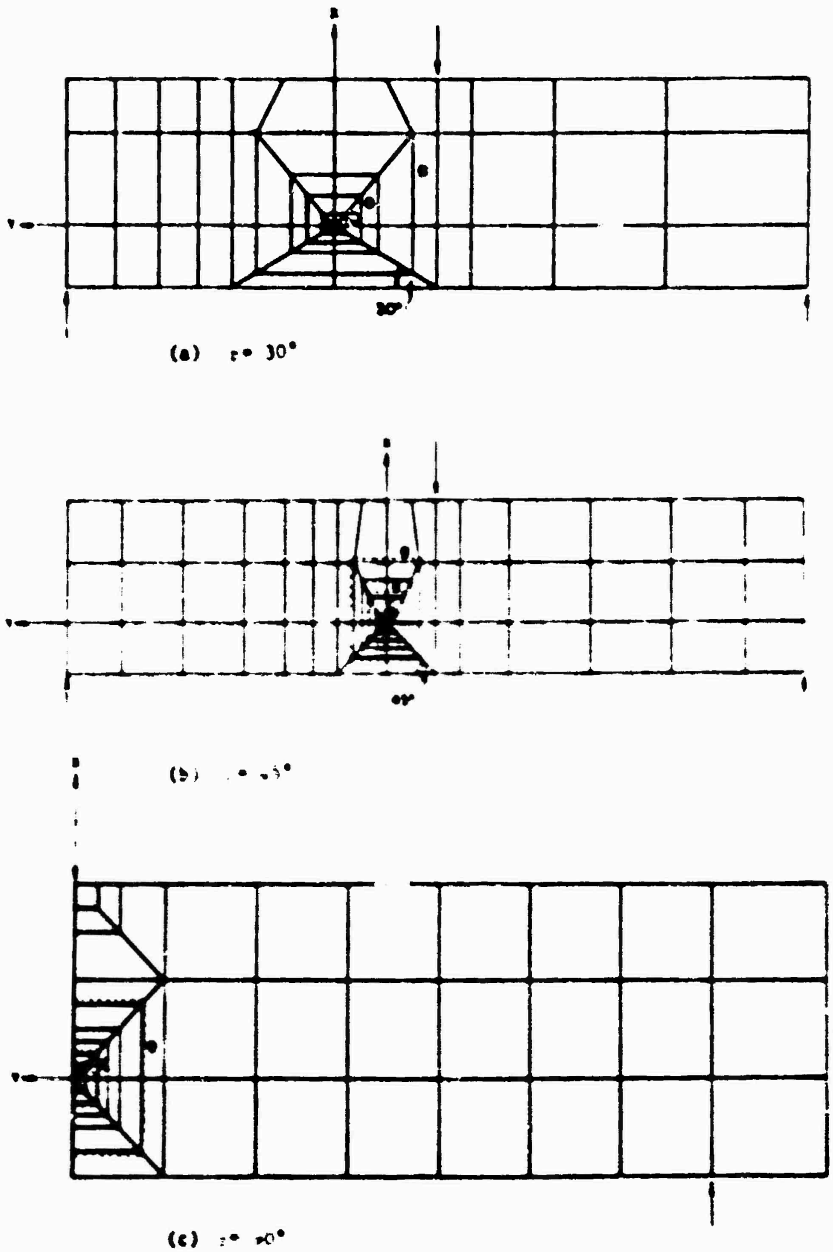

FIGURE 10. FINITE ELEMENT MESH FOR 30°, 45°, and 90° SPECIMENS

TABLE 5. $\hat{J}_1$ and $\hat{J}_2$ AT INITIATION FOR QUASI-STATIC LOADING

β	$\hat{J}_{1c}$ N/m	$-\hat{J}_{2c}$ N/m
30°	6.26×10^4	10.99×10^4
45°	12.84×10^4	12.5×10^4
90°	25.4×10^4	-

Using the results of Table 5 a plot of crack angle (β) vs. the $\hat{J}_1$ at initiation ($\hat{J}_{1c}$) was made. This is shown in Figure 11. An empirical fit of these data suggested that initiation occurs when

$$\hat{J}_1 = J_c \sin^2\beta \qquad (1)$$

where J_c is the critical value of $\hat{J}$ at β = 90°. Note that within the deformation theory of plasticity assumption, J_c coincides exactly with the $\hat{J}$-integral value at crack initiation.

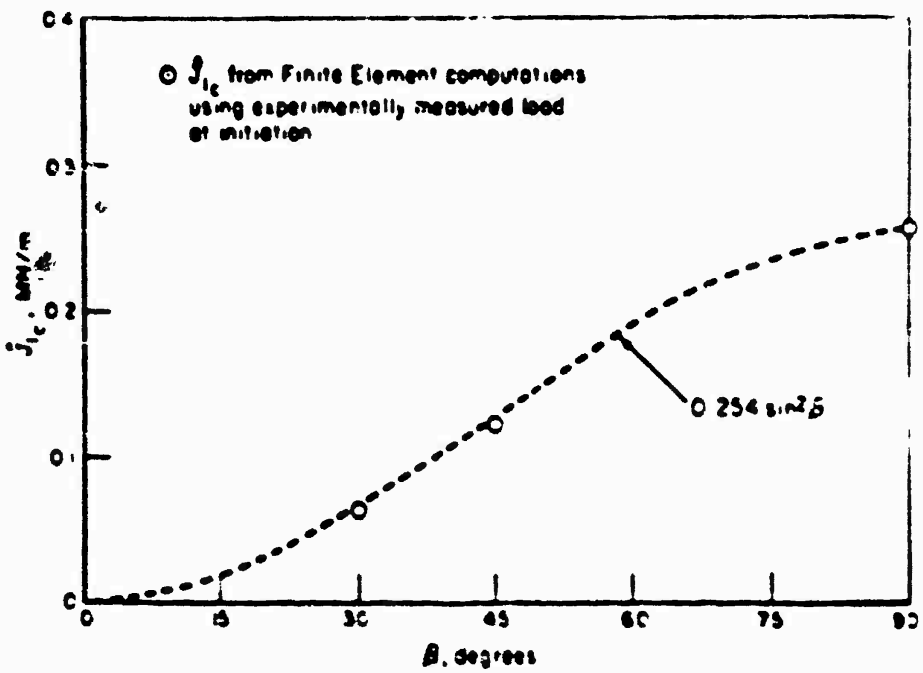

FIGURE 11. VARIATION OF $\hat{J}_{1c}$ WITH NOTCH ANGLE IN QUASI-STATIC LOADING

Turning now to impact loading conditions, a dynamic generalization of Equation (1) would be given by

$$\hat{J}_1 = DJ_c \sin^2\beta \qquad (2)$$

where $\hat{J}_1$ now contains inertia effects while D is a rate-dependent material constant. If the loading rate effect is small, then $D \approx 1$. The assumption will be made here on the basis that it is consistent with the use of the static stress-strain curve in finite element calculations. Therefore, strain-rate effects are omitted from both sides of Equation (2). Now, using Equation (2) and the results of dynamic finite element computations, a prediction of the time at which crack growth will initiate can be made. A comparison of these predictions with the experimentally measured time at initiation is contained in Figure 12. It can be seen that the prediction is quite reasonable.

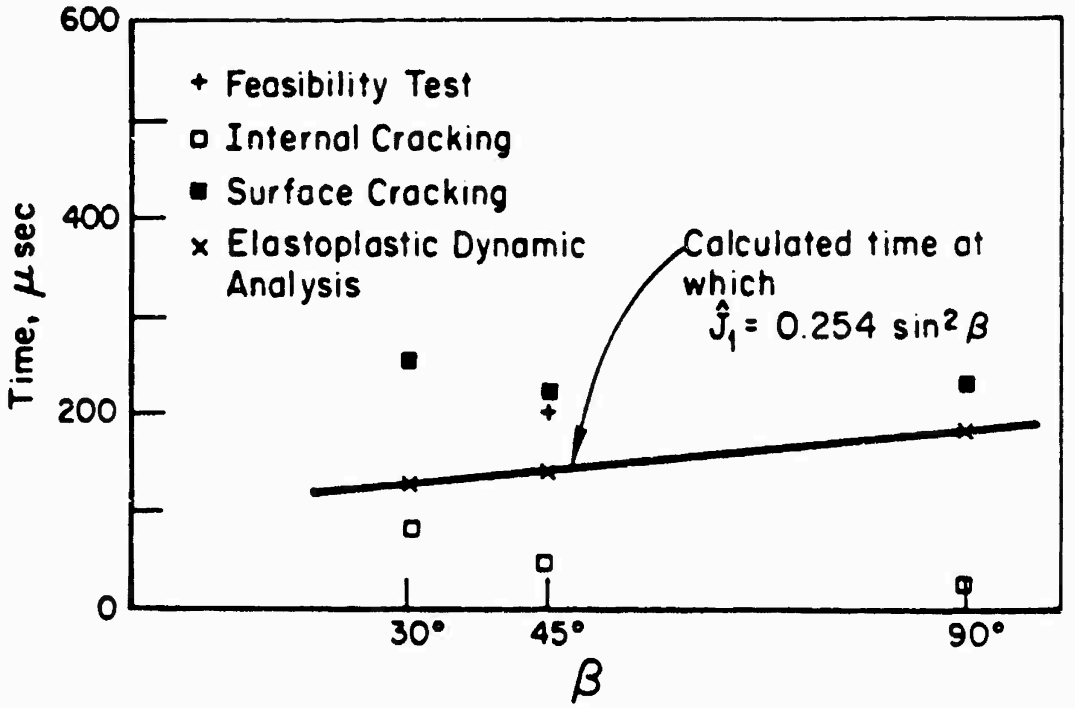

FIGURE 12. COMPARISON OF PREDICTED AND EXPERIMENTALLY MEASURED TIME AT INITIATION IN IMPACT LOADING

DISCUSSION OF RESULTS

The crack initiation criterion suggested by Equation (1) is based on fitting a curve through only four data points (three experimental results together with the origin). To explore the possibility that some other

function of β could provide just as good a fit, the problem depicted in Figure 13 was considered. This is an infinite plate containing a crack of length 2a that is subjected to a remote uniaxial applied stress whose direction makes an angle β with the crack line. The linear elastic solution of this problem gives [7]:

$$K_I = \sigma(\pi a)^{1/2} \sin^2\beta$$

and

$$K_{II} = \sigma(\pi a)^{1/2} \sin\beta\cos\beta. \tag{3}$$

The relation between $\hat{J}_1$ and the stress intensity factors K_I and K_{II} will give

$$\hat{J}_1 = \left\{\frac{k+1}{8}\sigma(\pi a)^{1/2}\right\}\sin^2\beta \tag{4}$$

where μ is the shear modulus, and $k = 3-4\nu$ for plane stress and $k = (3-\nu)/(1+\nu)$ for plane strain.

The expression within the brackets is the energy release rate G which, in a linear elastic problem, is just J. Therefore, Equation (4) can be written as

$$\hat{J}_1 = J \sin^2\beta \tag{5}$$

Now if fracture occurs when J achieves a critical value that is independent of β, then Equation (5) will be identical to Equation (1).

Despite their similarity, there is a significant difference between the origins of Equations (1) and (5). Specifically, Equation (5) contains $\hat{J}_1$ found by taking the material to be linear elastic and assuming a fracture criterion; i.e., $J = J_c$ for all β values. In contrast, Equation (1) was obtained by computing $\hat{J}_1$ by elastic-plastic finite element computations and using actual fracture data. Two conclusions can tentatively be drawn. First, the functional relationship between $\hat{J}_1$ and J in the linear elastic case may remain unaffected by plasticity. Second, this criterion may be geometry-independent. If indeed this is the case, the problem of predicting crack initiation reduces simply to knowing J_{1c} for the material and performing a linear elastic analysis of the problem to determine the relationship between J and $\hat{J}_1$. These implications present intriguing possibilities which must be further explored.

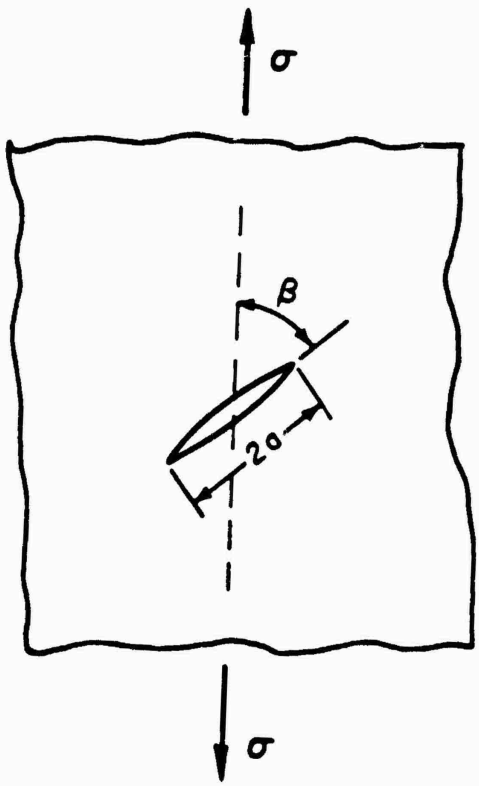

FIGURE 13. INFINITE PLATE WITH INCLINED CRACK

In regard to the prediction of crack initiation in impact loading, Figure 12 shows quite reasonable agreement. However, the significance of this observation is not certain at this time. The fact that the predicted time at initiation in all three cases lies within the measured time interval from the instant when the crack initiation was detected below the surface of the specimen to the instant when it appeared at the surface is very encouraging. That is, since the two-dimensional finite element analyses used in the prediction do not model crack tunnelling, the predicted time should be comparable to some instant inside the measured interval. While it can therefore be claimed that the experiments do provide data that are comparable to the analysis predictions, more experiments are needed to draw any decisive conclusions.

CONCLUSIONS

The results described in this paper indicate that the $\hat{J}$ parameter can be used as an effective criterion for crack initiation in elastic-plastic mixed mode loading conditions. Because a reasonable prediction was made for impact loading using quasi-statically-based values, it appears that the effect of loading rate may not be too important in HY-100 steel. Finally, the results suggest the intriguing possibility that the geometric influences on mixed mode loading under elastic-plastic conditions may be identical to those arising in linear elastic conditions.

ACKNOWLEDGEMENT

This work was performed for t'_ Naval Sea Systems Command via David Taylor Naval Ship Research and Development Center, Contract Number N00167-80-C-0253. The authors would like to express their appreciation to Nash Gifford and Archie Wiggs of DTS NRDC for their support and encouragement of this work.

REFERENCES

[1] Kanninen, M. F., Popelar, C. H., and Broek, D., "A Critical Survey on the Applications of Plastic Fracture Mechanics to Nuclear Pressure Vessels and Piping", Nuclear Engineering and Design, 67, 27-55, 1981.

[2] Kishomoto, K., Aoki, S., and Sakata, M., "On the Path Independent Integral J", Engineering Fracture Mechanics, Vol. 13, 841-850, 1980.

[3] Jung, J., Ahmad, J., Kanninen, M. F., and Popelar, C. H., "Finite Element Analysis of Dynamic Crack Propagation", Failure Prevention and Reliability - 1981, F.T.C. Loo, Editor, ASME, 1981.

[4] Ahmad, J., Jung, J., Barnes, C. R., and Kanninen, M. F., "The Development of a Dynamic Elastoplastic Finite Element Analysis for Fast Fracture Under Impact Loading", To appear in Engineering Fracture Mechanics.

[5] "Test for Dynamic Tear Energy of Metallic Materials", Annual Book of ASTM Standards, Part 10, Philadelphia, 1981.

[6] Kanninen, M. F., et al, "Dynamic Crack Propagation Under Impact Loading", Nonlinear and Dynamic Fracture Mechanics AMD, Vol. 35, N. Perrone and S. N. Atluri, Editors, The American Society of Mechanical Engineers, New York, 1979.

[7] Paris, P. C. and Sih, G. C., "Stress Analysis of Cracks", ASTM STP 381, p. 30, 1965.